UPGRADE PERC WITH TOPCON: EFFICIENCY POTENTIAL BY TAKING INTO ACCOUNT THE ELECTRICAL GAINS AND OPTICAL LOSSES

Christoph Messmer[1,2], Andreas Fell[1], Frank Feldmann[1], Jonas Schön[1,2], Martin Hermle[1]

[1]Fraunhofer Institute for Solar Energy Systems ISE, Heidenhofstraße 2, 79110 Freiburg, Germany
[2]Laboratory for Photovoltaic Energy Conversion, University of Freiburg, Emmy-Noether-Straße 2, 79110 Freiburg, Germany
Phone: +49 761 203 54176 | e-mail: christoph.messmer@ise.fraunhofer.de

ABSTRACT: Passivating contacts like the tunnel-oxide passivating contact (TOPCon) technology are promising candidates for a next generation of silicon solar cells and are currently being implemented in industrial cell manufacturing. Since there are a number of possibilities how to integrate TOPCon via various cell architectures into industrial cells, it demands educated decisions to direct R&D efforts into the most promising candidates, i.e. creating a roadmap based on expected performance gains. This work shows how to thoroughly quantify the performance potential via numerical device simulation. Focus of this work is an evolutionary upgrade of the current PERC technology, that is introducing TOPCon on the rear and front side to reduce contact recombination but sticking to a p-type wafer and phosphorus diffused emitter. We specifically highlight the need to fully consider not only the electrical gains, but also the substantial optical losses through parasitic absorption in the poly silicon layers. A moderate efficiency gain of below $1\%_{abs}$ with respect to the current PERC technology is found. However, this gain may, counterintuitively, increase in future along with an improved PERC technology, if emitter and bulk recombination as the dominating losses can be reduced.

Keywords: Passivating contacts, TOPCon, Roadmap, Simulation, Parasitic absorption, Free-carrier absorption, Sentaurus TCAD, Quokka

1 INTRODUCTION

Passivating contacts like the tunnel-oxide passivating contact (TOPCon [1]) technology are currently being evaluated for their suitability for mass production. The high potential of TOPCon and similar technologies has been proven by efficiency potentials of laboratory solar cells reaching ~26% [2, 3]. The key question for this promising technology is how to integrate TOPCon into industrial process sequences. There are a number of possibilities how to integrate TOPCon via various cell architectures into industrial cell. One approach is to apply TOPCon in an evolutionary manner to the PERC technology by either substituting the full rear side with p-type TOPCon, and/or by substituting the local phosphorus emitter by n-TOPCon on the front side. This might require the fewest changes to the current standards of industrial PERC mass production by sticking to p-type bulk material and a phosphorus diffused front emitter. A more disruptive change not investigated in this paper would be to replace the bulk material by n-type c-Si and using a boron doped front emitter, which is one path currently applied in industry [4].

To make educated decisions and direct investment into the most promising candidates, a roadmap based on expected performance gains is essential. This work shows how to quantify the performance potential via numerical device simulation. The methodology of previous roadmaps [5, 6] is extended by focusing on both electrical gains and also the associated optical losses. We will focus on evolutionary TOPCon upgrades of a high efficiency bifacial PERC solar cell on p-type Cz wafers with screen-printed metallization and a zero busbar concept with properties realistically achievable in industrial manufacturing. We explicitly consider the parasitic absorption (including free carrier absorption) within the poly silicon layers which (partly) compensate the electrical gains. For the experimental verification of the optical simulation model and further details we refer to [7].

2 SIMULATION METHOD

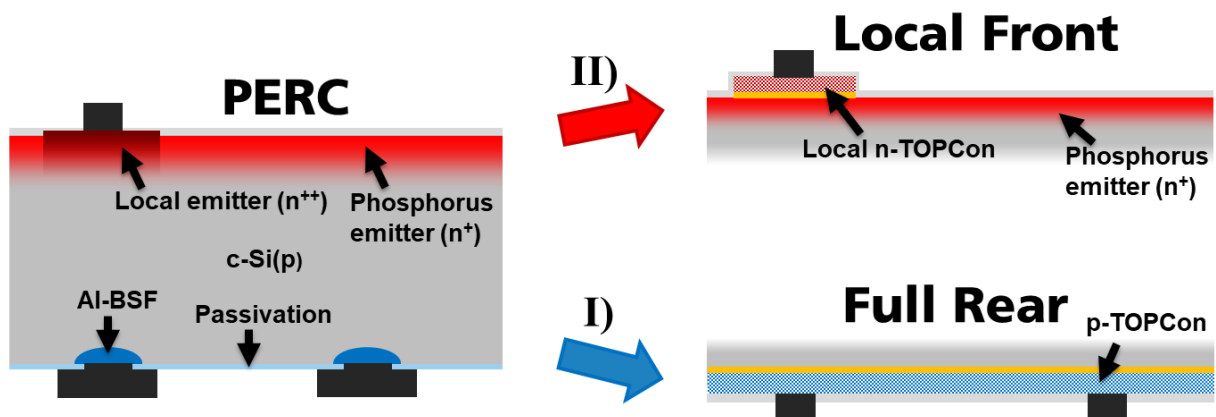For optical modelling of the cell architectures we use

Figure 1: Investigated cell architectures. On the left: A standard industrial PERC cell as reference. On the right: Two TOPCon upgrade architectures: I) Full Rear: Full-area rear p-type TOPCon with rear dielectric and local contact openings. II) Local Front: n-type TOPCon locally aligned to front contacts. A combination of I and II yields the final upgraded cell.
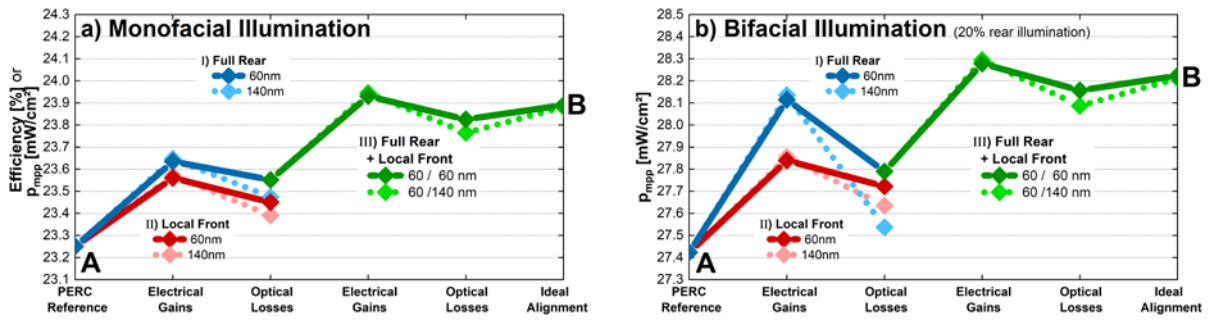
Figure 2: Roadmaps showing the power at maximum-power-point (MPP) for a zero busbar design starting from a PERC reference cell (cell A) under (a) only front illumination of one sun or (b) additional 20% rear illumination (bifacial illumination). The electrical gains and optical losses (including free-carrier absorption, FCA) are separately shown for two different poly silicon layer thicknesses (solid for 60nm, dotted for 140nm).

the raytracer of Sentaurus TCAD [8]. All thin-layers at the front and rear side are modelled with transfer-matrix-method, which takes into account refraction and parasitic band-to-band and free-carrier absorption (FCA) of the incoming light. The FCA in the c-Si bulk and poly-silicon layers is described according to Baker-Finch [9, 10]. For bifacial application we assume simultaneous illumination of 20% Am1.5g from the rear side. For details of the optical model and experimental verification we refer to [7].

The electrical modeling of the cell architectures was done with Quokka3 [11, 12] using a 'zero busbar' symmetry element. Thus, the finger resistance as well as busbar shading is neglected, essentially assuming a busbar-less interconnection concept.

Figure 1 on the left shows a bifacial PERC cell which is used as a reference and starting point with 23.25% efficiency for front illumination representing a high-end industrial solar cell with zero busbar design. As bulk material we assume a p-type Cz material with 1 Ωcm and minority carrier lifetime of 1 ms. The front side is featuring a phosphorus diffused front emitter (J_0=30 fA/cm², R_S=150 $\Omega/\square$, [13]), a highly doped local emitter with a width of 145 µm and a 45 µm metal contact (J_0=800 fA/cm², [6]). The rear side is fully passivated with AlOx/SiNx (J_0=10 fA/cm²) featuring local Al-BSF contacts (J_0=400 fA/cm², [5, 13]). For all cell structure variations the front and rear finger pitch was optimized in order to reach the highest efficiency.

Proceeding from this PERC cell reference (Fig. 1, left) we investigate two TOPCon upgrades as shown in Fig. 1 on the right:
I) Full Rear is featuring a full-area rear p-type TOPCon with a poly silicon thickness of 60 or 140 nm (R_S = 320 or 137$\Omega/\square$, $J_{0,pass,p-TOPCon}$ = 5 fA/cm² [14, 15]) and with a rear dielectric and local contacts with slightly higher recombination ($J_{0,met}$ = 20 fA/cm²). Since TOPCon allows for screen-printing of Ag-fingers instead of Al, we take the same finger width of 45 µm as on the front side. The FCA in the poly layer was experimentally verified in [7].
II) Local Front features an n-type TOPCon with a **poly**-Si thickness of 60 or 140 nm aligned to the front contact (w_{TOPCon} = 135 µm, $w_{Contact}$ = 45 µm). Due to screen-printing of the metal we assumed the recombination underneath the contact to be $J_{0,met,n-TOPCon}$ = 20 fA/cm².

3 RESULTS

3.1 Efficiency Potential of TOPCon Upgrades on PERC

In the following we showcase the roadmaps highlighting electrical gains and optical losses. Figure 2a shows the efficiency (or power output density at maximum power point p_{mpp}) for the cell structures presented in Fig. 1 for one sun front illumination. Starting from the 23.25% efficiency for the PERC reference cell, we first apply the full rear p-TOPCon upgrade as introduced in Fig. 1 (I). The solid blue line shows the electrical gain and optical loss for a poly-Si(p) thickness of 60 nm. One can see that an electrical gain of about 0.4%$_{abs}$ which is than partly compensated by optical losses of about 0.1%$_{abs}$ due to free-carrier absorption (FCA) in the poly-Si layer. A thicker poly-Si layer of 140 nm (see blue dotted line in Fig. 2a) has only a negligible electrical benefit due to lateral conductivity in the poly-Si, however, the FCA increases which leads to higher efficiency losses than for thin poly-Si.

For the local front n-TOPCon upgrade (shown in red) with an alignment tolerance of one finger width on both sides of the metal finger (45 µm), we get an electrical gain in efficiency which is similarly high as for the full rear (~0.3%$_{abs}$), however, approximately half of the electrical gains are compensated by optical losses. The optical losses on the front side are dominated by parasitic absorption of light with short wavelengths, whereas FCA plays a secondary role. Notably, this optical loss can be reduced by improving the alignment and thus reducing the width of the local TOPCon region beneath the metal finger.

Proceeding from full rear with 60 nm p-TOPCon on the rear, we additionally apply the local front n-TOPCon upgrade (shown in green) to get the fully TOPCon upgraded p-PERC cell (cell B in Fig. 2a). Again, the electrical gains (~0.4%$_{abs}$) are partly compensated by optical losses (~0.1-0.2%$_{abs}$), whereby its absolute number depends on the poly-Si(n) thickness (solid green for 60 nm, dotted green for 140 nm) and the alignment tolerance (135 µm n-TOPCon as standard). The last step shows the influence of ideal alignment, where the poly-Si(n) is perfectly aligned to the metal fingers with a width of 45 µm. For the monofacial illumination in Fig. 2a we end up with an overall efficiency gain of about 0.65%$_{abs}$.

We emphasize that the absolute numbers of these electrical gains and optical losses depend on the initial reference cell and parameter assumptions (e.g. $J_{0,met}$). Therefore this roadmap should be fine-tuned individually for a specific PERC cell reference and experimentally
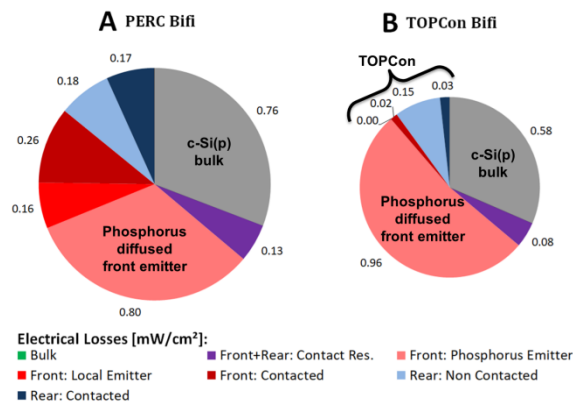
Figure 3: Electrical loss analysis (FELA) for both PERC (cell A) and TOPCon on both sides (cell B) under bifacial illumination.

realized properties of the TOPCon features.

Since bifacial applications of solar cells become even more important in the future, we show the same roadmap with additional rear illumination of 200 W/m² of AM1.5g spectrum in Fig. 2b. One can see that this roadmap starts with a maximum output power P_{mpp} of 27.4 mW/cm² for the PERC reference. When applying the TOPCon upgrades, first, we see that for the full rear (shown in blue) the electrical gain is higher than for the local front (shown in red). However, also the optical losses are higher for full rear due to additional parasitic absorption of light from the rear side in the full-area TOPCon layer for short wavelengths (in addition to FCA). We can see that it highly depends on the illumination setup and the choice of cell parameters, whether Full Rear or Local Front is a better option for a first evolutionary step towards a TOPCon based industrial cell. However, in any case, Fig. 2 highlights that optical losses are substantial and should be quantitatively taking into account when we want to make a reasonable choice on the next evolutionary steps of the PERC cell technology towards passivating contacts like TOPCon.

3.2 Electrical limitations

Figure 3 on the left shows the electrical losses (FELA) of the p-PERC reference cell under bifacial illumination as a pie chart (corresponds to cell A in Fig. 2b). One can see that the c-Si(p) bulk (shown in grey) and phosphorus diffused front emitter (shown in light red) already account for about a third of the electrical losses each. Another third is accounted for by the front side (selective emitter and metallized selective emitter, shown in red and dark red, respectively), rear side (light blue for passivation, dark blue for contacted aluminum BSF) and contact resistivities (front and rear, shown in purple, not further considered, see [7]).

Figure 3 on the right shows the electrical loss analysis for the final upgraded cell architecture (cell B in Fig. 2b). The total electrical losses were lowered by about 25% compared to PERC, and the two TOPCon upgrades on the front and rear minimized the corresponding electrical losses to a share of about 10% (see brace in Fig. 3).

These pie charts explain the only moderate efficiency gains of the roadmaps in Fig. 2. The PERC cell used as a reference was chosen as high-end industry cell whose electrical losses are already dominated by p-PERC specific features like the c-Si(p) bulk and phosphorus front emitter (up to two thirds). When optimizing only
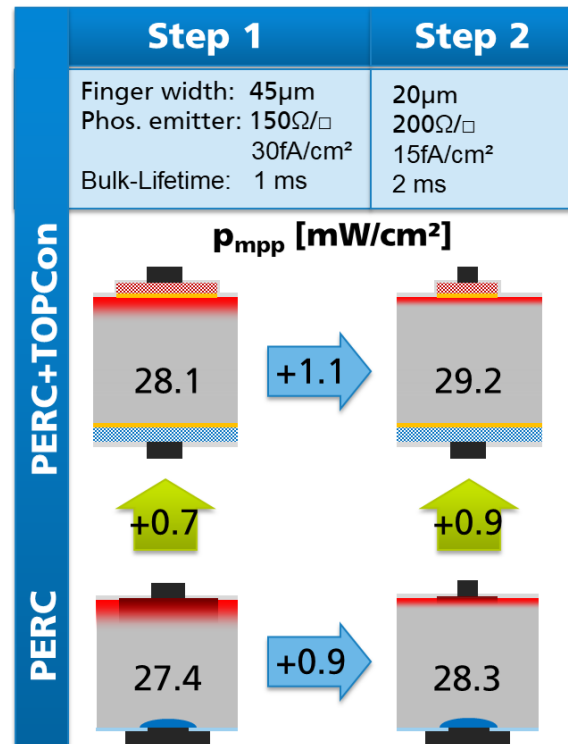

Figure 4: Simulated power output density p_{mpp} for both PERC and TOPCon-upgraded cell. Step 1 shows the parameters used in this paper, step 2 shows a possible development of PERC technology in the future. The green and blue arrows show the power gains for TOPCon upgrade and future PERC development, respectively.

the remaining third of the electrical losses by TOPCon, the corresponding shares go down to a minimum, however, the final cell is now almost completely dominated by p-PERC specific features.

3.3 Benefits from further PERC Developments

A more substantial efficiency improvement seems to be only possible by improvement of the phosphorus emitter or a change to n-type silicon bulk material (with a boron emitter and full-area rear n-TOPCon), the latter being the current focus of industrialization. However, the evolutionary approach of upgrading p-PERC by TOPCon benefits from the ongoing development of the PERC technology, in particular improvements in bulk and emitter recombination, the latter being linked to achievable finger-width by allowing higher emitter sheet resistance. Figure 4 shows an example of how this influences the TOPCon upgrades as shown in this paper. Starting from the left (Step 1), we see the PERC reference (down) and the TOPCon upgraded cell (up) and their corresponding power density p_{mpp} at maximum power point under bifacial illumination (p_{mpp}=27.4 mW/cm² and 28.1 mW/cm² for PERC and TOPCon upgraded cell, respectively). The difference of 0.7 mW/cm² is according to Fig. 2b.

Now assume, the p-PERC process sequence will profit from future developments like shown for step 2, including smaller Ag finger widths of 20 µm, a minority lifetime of 2 ms and a phosphorus emitter with sheet resistance R_S=200 Ω/□ and J_0=15fA/cm². This exemplary future improvement will boost the p-PERC cell by 0.9 mW/cm² (blue arrow) to 28.3 mW/cm². However, the TOPCon upgraded PERC cell automati-

cally benefits from the same development, boosting its power density by 1.1 mW/cm² to 29.2 mW/cm². One can see that the TOPCon upgraded cell benefits more (1.1 compared to 0.9 mW/cm^2) than the p-PERC cell due to synergy effects.

4 SUMMARY

In this paper we investigated the effect of evolutionary TOPCon upgrades on the mainstream PERC technology. We highlighted the importance to fully take into account the optical effects in order to obtain (more) reliable efficiency predictions from simulation. We showcased an evolutionary roadmap from PERC by including TOPCon technologies on the front and/or rear side, where both electrical gains and optical losses were differentiated. The latter especially included free-carrier absorption which was verified by experiments in [7]. It showed that TOPCon upgrades yield the expected electrical gains due to reduced contact recombination, which however are substantially lowered by the introduced parasitic absorption in the polysilicon layers resulting in an overall gain of somewhat below 1%$_{abs}$. The loss analysis on the final cell reveals that its efficiency is limited by the phosphorus diffused front emitter and p-type bulk to below 24%. However, we showcased that the efficiency gain of TOPCon upgrades may, counterintuitively, increase in future along with an improved PERC technology, if emitter and bulk recombination as the dominating losses can be reduced. We therefore conclude that such an evolutionary upgrade may well be an attractive option in the future, along with the current mainstream of switching to n-type bulk material and a boron doped emitter.

5 ACKNOWLEDGMENT

6 REFERENCES

[1] F. Feldmann, M. Bivour, C. Reichel, H. Steinkemper, M. Hermle, and S. W. Glunz, "Tunnel oxide passivated contacts as an alternative to partial rear contacts," *Sol. Energy Mater. Sol. Cells*, vol. 131, pp. 46–50, 2014.

[2] A. Richter, J. Benick, F. Feldmann, A. Fell, M. Hermle, and S. W. Glunz, "n-Type Si solar cells with passivating electron contact: Identifying sources for efficiency limitations by wafer thickness and resistivity variation," *Sol. Energy Mater. Sol. Cells*, vol. 173, pp. 96–105, 2017.

[3] F. Haase, C. Hollemann, S. Schäfer, A. Merkle, M. Rienäcker, J. Krügener, R. Brendel, and R. Peibst, "Laser contact openings for local poly-Si-metal contacts enabling 26.1%-efficient POLO-IBC solar cells," *Sol. Energy Mater. Sol. Cells*, vol. 186, pp. 184–193, 2018.

[4] Y. Chen, D. Chen, C. Liu, Z. Wang, Y. Zou, Y. He, Y. Wang, L. Yuan, J. Gong, and W. Lin, "Mass production of industrial tunnel oxide passivated contacts (i-TOPCon) silicon solar cells with average efficiency over 23% and modules over 345 W," *Prog. Photovolt: Res. Appl.*, 2019.

[5] B. Min, M. Muller, H. Wagner, G. Fischer, R. Brendel, P. P. Altermatt, and H. Neuhaus, "A Roadmap Toward 24% Efficient PERC Solar Cells in Industrial Mass Production," *IEEE J. Photovoltaics*, vol. 7, no. 6, pp. 1541–1550, 2017.

[6] L. Tous *et al., Eds., Efficiency Roadmaps for Industrial Bifacial pPERC and nPERT Cells.* SiliconPV 2019, Leuven.

[7] C. Messmer, A. Fell, F. Feldmann, N. Woehrle, J. Schön, and M. Hermle, "Efficiency Roadmap for Evolutionary Upgrades of PERC Solar Cells by TOPCon: Impact of Parasitic Absorption," 2019.

[8] Synopsis, "Sentaurus Device User Guide: release L-2016.03-SP2," http://www.synopsys.com, 2016.

[9] S. C. Baker-Finch, K. R. McIntosh, D. Yan, K. C. Fong, and T. C. Kho, "Near-infrared free carrier absorption in heavily doped silicon," *J. Appl. Phys.*, vol. 116, no. 6, p. 63106, 2014.

[10] F. Feldmann, M. Nicolai, R. Müller, C. Reichel, and M. Hermle, "Optical and electrical characterization of poly-Si/SiO x contacts and their implications on solar cell design," *Energy Procedia*, vol. 124, pp. 31–37, 2017.

[11] A. Fell, *quokka3*. [Online] Available: www.quokka3.com. Accessed on: Jan. 22 2018.

[12] A. Fell, J. Schön, M. C. Schubert, and S. W. Glunz, "The concept of skins for silicon solar cell modeling," *Sol. Energy Mater. Sol. Cells*, vol. 173, pp. 128–133, 2017.

[13] A. Fell and P. P. Altermatt, "A Detailed Full-Cell Model of a 2018 Commercial PERC Solar Cell in Quokka3," *IEEE Journal of Photovoltaics*, vol. 8, no. 6, pp. 1443–1448, 2018.

[14] U. Römer, R. Peibst, T. Ohrdes, B. Lim, J. Krugener, T. Wietler, and R. Brendel, "Ion Implantation for Poly-Si Passivated Back-Junction Back-Contacted Solar Cells," (English), *IEEE J. Photovoltaics*, vol. 5, no. 2, pp. 507–514, 2015.

[15] P. Padhamnath, J. Wong, B. Nagarajan, J. K. Buatis, L. M. Ortega, N. Nandakumar, A. Khanna, V. Shanmugam, and S. Duttagupta, "Metal contact recombination in monoPoly™ solar cells with screen-printed & fire-through contacts," *Solar Energy Materials and Solar Cells*, vol. 192, pp. 109–116, 2019.